Magnetic interactions in the multiferroic phase of $CuFe_{1-x}Ga_xO_2$ ($x = 0.035$) refined by inelastic neutron scattering with uniaxial-pressure control of domain structure

Taro Nakajima[*] and Setsuo Mitsuda

Department of Physics, Faculty of Science, Tokyo University of Science, Tokyo 162-8601, Japan

Jason T. Haraldsen

Theoretical Division, Los Alamos National Laboratory, Los Alamos, New Mexico 87545, USA and Center for Integrated Nanotechnologies, Los Alamos National Laboratory, Los Alamos, New Mexico 87545, USA

Randy S. Fishman

Material Science and Technology Division, Oak Ridge National Laboratory, Oak Ridge, Tennessee 37831, USA

Tao Hong

Quantum Condensed Matter Division, Oak Ridge National Laboratory, Oak Ridge, Tennessee 37831, USA

Noriki Terada

National Institute for Materials Science, Tsukuba, Ibaraki 305-0047, Japan

Yoshiya Uwatoko

Institute for Solid State Physics, University of Tokyo, Kashiwa, Chiba 903-0213, Japan

We have performed inelastic neutron scattering measurements in the ferroelectric noncollinear-magnetic phase of $CuFe_{1-x}Ga_xO_2$ (CFGO) with $x = 0.035$ under applied uniaxial pressure. This system has three types of magnetic domains with three different orientations reflecting the trigonal symmetry of the crystal structure. To identify the magnetic excitation spectrum corresponding to a magnetic domain, we have produced a nearly "single-domain" multiferroic phase by applying a uniaxial pressure of 10 MPa onto the [$1\bar{1}0$] surfaces of a single-crystal CFGO sample. As a result, we have successfully observed the single-domain spectrum in the multiferroic phase. Using the Hamiltonian employed in the previous inelastic neutron scattering study on the "multi-domain" multiferroic phase of CFGO ($x = 0.035$) [Haraldsen *et al*. Phys. Rev. B **82**, 020404(R) (2010)], we have refined the Hamiltonian parameters so as to simultaneously reproduce both of the observed single-domain and multidomaim spectra. Comparing between the Hamiltonian parameters in the multiferroic phase of CFGO and in the collinear four-sublattice magnetic ground state of undoped $CuFeO_2$ [Nakajima *et al*., Phys. Rev. B **84**, 184401 (2011)], we suggest that the nonmagnetic substitution weakens the spin-lattice coupling, which often favors a collinear magnetic ordering, as a consequence of the partial release of the spin frustration.

I. INTRODUCTION

A triangular lattice antiferromagnet $CuFeO_2$ (CFO) is known as a spin-driven magneto-electric multiferroic.[1] While the ground state of CFO is a *nonferroelectric* collinear four-sublattice (4SL) magnetic phase with a magnetic modulation wave vector of $(\frac{1}{4},\frac{1}{4},\frac{3}{2})$,[2] the spin-driven ferroelectricity appears in the first magnetic-field induced phase from the 4SL phase.[1] By substituting only a few percent of nonmagnetic ions (Al^{3+}, Ga^{3+}, or Rh^{3+}) for the magnetic Fe^{3+} sites, the transition field from the 4SL phase to the multiferroic phase is readily reduced down to zero field;[3–6] for example, in $CuFe_{1-x}Ga_xO_2$ (CFGO) with $x = 0.035$, the 4SL phase disappears, and instead the multiferroic phase shows up as a ground state.[5] This implies that the 4SL and the multiferroic phases are almost degenerate in energy owing to the magnetic frustration in this system, and thus a small perturbation such as a few percent of nonmagnetic substitution can affect the magnetic ground state. Previous elastic neutron scattering measurements using CFGO and $CuFe_{1-x}Al_xO_2$ (CFAO) samples have revealed that the magnetic structure in the multiferroic phase is a screw-type structure having a magnetic modulation wave vector of $(q,q,\frac{3}{2})$ with $q = 0.203$.[7,8] Recent theoretical studies by Haraldsen *et al*. have pointed out that the turn angles of the screw-type helical arrangement of the spins have anharmonicity.[9,10]

To elucidate how a small amount of nonmagnetic substitution changes the magnetic ground state of this system, it is important to determine the Hamiltonian parameters in both of the 4SL and multiferroic phases. In a previous study, Ye *et al*. have performed inelastic neutron scattering measurements on CFO to determine the parameters in the 4SL phase.[11] They have observed spin-wave excitation spectra in the multi-domain 4SL phase, in which three types of magnetic domains with modulation wave vectors of $(\frac{1}{4},\frac{1}{4},\frac{3}{2})$, $(\frac{1}{4},-\frac{1}{2},\frac{3}{2})$, and $(-\frac{1}{2},\frac{1}{4},\frac{3}{2})$ coexist. The formation of these three domains is due to the trigonal symmetry of the original crystal structure of CFO. Hence the magnetic excitation spectra observed in the multi-domain 4SL phase are mixtures of the spectra arising from the three domains having the different orientations.
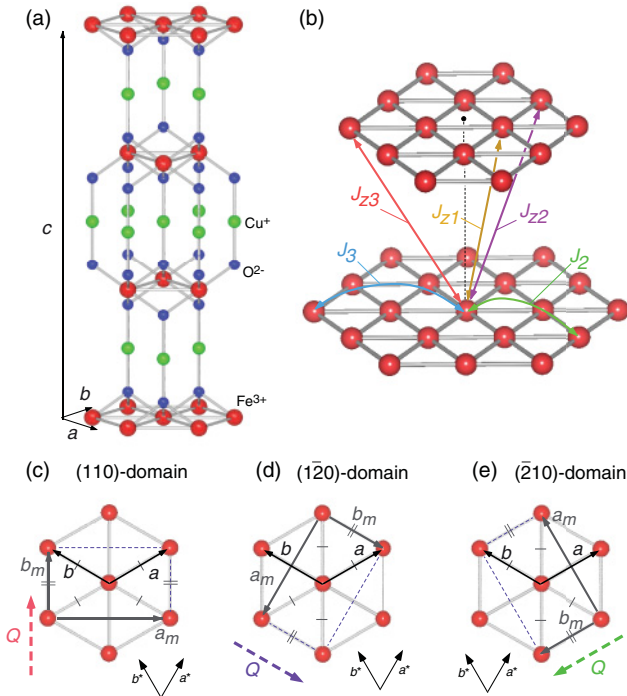
FIG. 1. (Color online) (a) Crystal structure of $CuFeO_2$ with a hexagonal basis. (b) Paths of the exchange interactions. For the nearest-neighbor exchange interactions, J_1, see Figs. 4(a) and 4(b). (c)–(e) The three types of magnetic domains with the monoclinic bases ($\boldsymbol{a}_m, \boldsymbol{b}_m$) and the hexagonal bases ($\boldsymbol{a}, \boldsymbol{b}$). Dashed arrows denote c^*-plane projections of the magnetic modulation wave vectors in each domain.

On the other hand, Nakajima *et al.* have recently demonstrated that volume fractions of the three domains can be controlled by application of uniaxial pressure.[12,13] Since the formation of the three magnetic domains accompanies with monoclinic lattice distortions in each domain as illustrated in Figs. 1(c)–1(e), an application of uniaxial pressure, which is directly coupled with the lattice degree of freedom, results in significant changes in the volume fractions of the magnetic/crystal domains. Actually, in Ref. 13, a single-domain 4SL phase is achieved by applying a uniaxial pressure of only 10 MPa onto the [1$\bar{1}$0] surfaces of the single-crystal CFO sample. Recent inelastic neutron scattering measurements using the slightly pressurized CFO sample have successfully identified the spin-wave dispersion relations belonging to a magnetic domain in the 4SL phase.[14] Starting from the Hamiltonian used in the previous theoretical spin-wave analysis by Fishman,[15] Nakajima *et al.* have refined the parameters, so as to reproduce the spin-wave dispersions in both of the single- and multi-domain 4SL states.[14]

As for the multiferroic phase, Haraldsen *et al.* have recently performed inelastic neutron scattering measurements using CFGO ($x = 0.035$) samples, and have deduced the Hamiltonian parameters from magnetic excitation spectra in the multi-domain multiferroic phase.[9] In the present study, we have performed inelastic neutron scattering measurements on CFGO ($x = 0.035$) under applied uniaxial pressure, in order to observe single-domain magnetic excitation spectra, from

which we can more accurately determine the Hamiltonian parameters in the multiferroic phase.

II. EXPERIMENTAL DETAILS AND PRELIMINARY RESULTS

Single crystals of CFGO ($x = 0.035$) of nominal compositions were grown by the floating zone method.[16] Before the present measurements with uniaxial pressure, we have performed inelastic neutron scattering measurements in the multi-domain multiferroic phase using three as-grown crystals (total mass 4.8 g). We used a triple-axis neutron spectrometer HER(C1-1) at JRR-3, Japan Atomic Energy Agency. The energy of the scattered neutrons was fixed at $E_f = 3.5$ meV, and the horizontal collimation was open 80'-80'-80'. The three single-crystal CFGO ($x = 0.035$) samples were co-aligned and mounted in a pumped ^{4}He cryostat with the (H, H, L) scattering plane. Figure 2(b) shows the magnetic excitation spectrum along the $(H, H, \frac{3}{2})$ line at 2.0 K in the multiferroic phase. We have confirmed that the observed spectrum is the same as that in previous measurements by Haraldsen *et al.*[9]

After this measurement, we cut one of the three crystals into a plate shape ($3.0 \times 3.2 \times 17$ mm^3) with the widest surfaces normal to the [1$\bar{1}$0] direction. The mass of the plate-shaped sample is 0.9 g. The sample was set into a uniaxial pressure cell, which is almost the same as the pressure cells used in Refs. 13, 14, and 17. A uniaxial pressure of 10 MPa was applied on the [1$\bar{1}$0] surfaces of the sample at room temperature, and was kept throughout the present experiment by CuBe disk springs set in the bottom of the pressure cell. We have performed inelastic neutron scattering measurements using the pressurized CFGO sample at another cold neutron triple-axis spectrometer CTAX(CG-4C) at the High Flux Isotope Reactor (HFIR), Oak Ridge National Laboratory. The pressure cell was loaded into a pumped ^{4}He cryostat with the (H, H, L) scattering plane. The energy of the scattered neutrons was mainly fixed at $E_f = 4.0$ meV. To measure the excitation spectra below 0.5 meV, we also used $E_f = 2.9$ meV. The energy resolutions at elastic conditions in the measurements with $E_f = 4.0$ and 2.9 meV are 0.2 and 0.1 meV (full width at half maximum), respectively. The higher-order contaminations were removed by a cooled Be filter placed between the sample and the analyzer.

III. EXPERIMENTAL RESULTS

We have estimated the volume fractions of the three magnetic domains, in the same manner as in Ref. 12. Using the notations in Ref. 12, we refer to the three domains as (110), (1$\bar{2}$0), and ($\bar{2}$10) domains [see Figs. 1(c)–1(e)]. In the multiferroic phase at 2 K, we have measured integrated intensities of three magnetic Bragg reflections located on (or near) the (H, H, L) scattering plane; specifically $(q, q, \frac{3}{2})$, $(\frac{1}{2} - q, 2q, \frac{1}{2})$, and $(2q, \frac{1}{2} - q, -\frac{1}{2})$ reflections, which belong to the (110), (1$\bar{2}$0), and ($\bar{2}$10) domains, respectively. Comparing the observed integrated intensities with the calculated structure factors for these reflections, we have determined the volume fraction of the (110), (1$\bar{2}$0), and ($\bar{2}$10) domains as 0.78, 0.09, and 0.13, respectively. This indicates that the (110) domain,
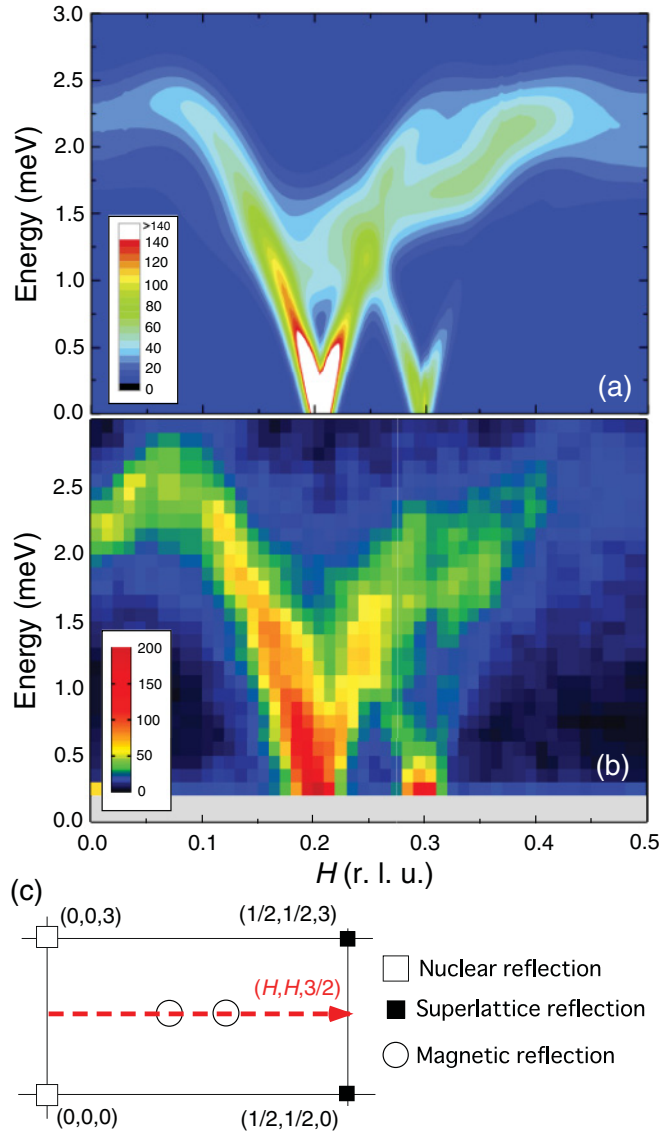
FIG. 2. (Color online) (a) Calculated and (b) observed intensity map of the magnetic excitation spectra along the $(H,H,\frac{3}{2})$ line in the multi-domain multiferroic phase. (c) Reciprocal-lattice map of the (H,H,L) scattering plane. The dashed arrow denotes the direction of the the $(H,H,\frac{3}{2})$ line.

FIG. 3. (Color online) (a) Calculated and (b) observed intensity map of the magnetic excitation spectra along the $(H,H,\frac{3}{2})$ line in the single-domain multiferroic phase. (c),(d) Profiles of the constant-E scans below 0.5 meV around (c) $H = 0.2$ and (d) 0.3.

whose propagation wave vector of $(q,q,\frac{3}{2})$ lies in the (H,H,L) scattering plane, dominates over the others.

In the (nearly) single-domain multiferroic phase at 2 K, we have performed constant-wave-vector (constant-q) scans with $E_f = 4.0$ meV, and have obtained an intensity map along the $(H,H,\frac{3}{2})$ line as shown in Fig. 3(b). We have found that intensities around $H \approx 0.3$ and $E \approx 1.7$ meV are reduced in the single-domain state, as compared to those in the multi-domain state. This is consistent with the previous calculation by Haraldsen *et al.*;[9] they have pointed out that the intensities around $H \approx 0.3$ and $E \approx 1.7$ meV are attributed to the magnetic excitation spectra arising from the $(1\bar{2}0)$ and $(\bar{2}10)$ domains. We also found that the intensities around the shoulder at $H \approx 0.08$ are also reduced in the single-domain state. While the previous calculation has suggested that the
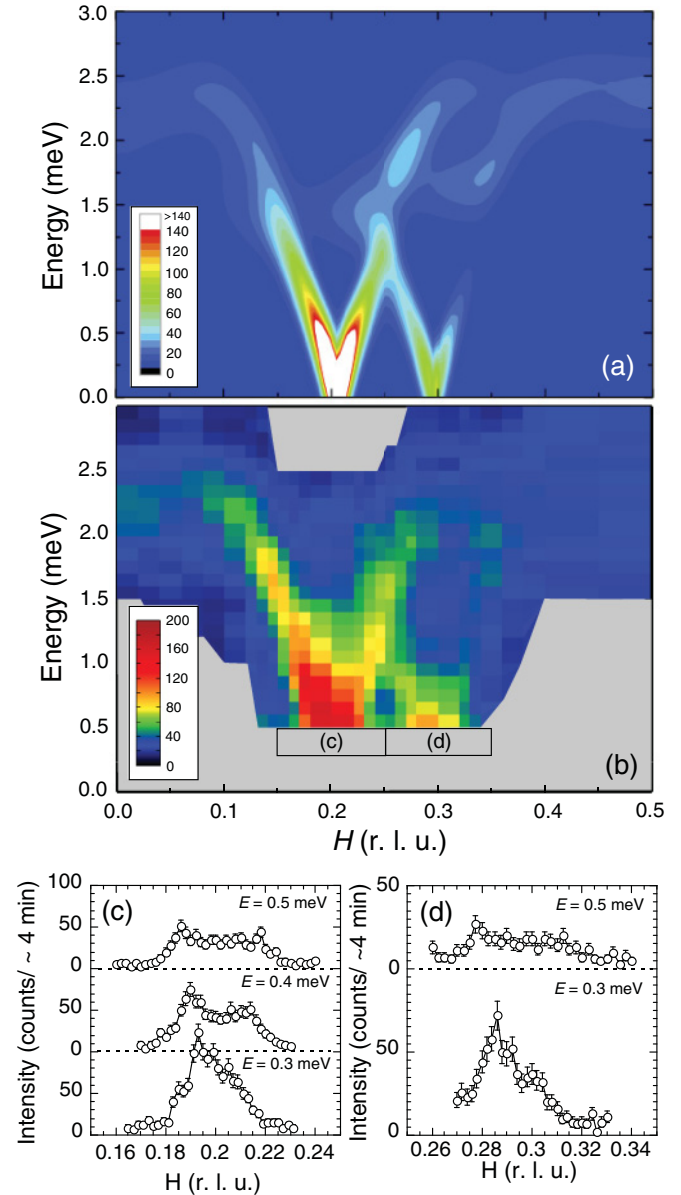
shoulder belongs to the (110) domain,[9] the present results indicate that it belongs to the other two domains.

To investigate the low-energy magnetic excitations below 0.5 meV, we have performed constant-energy-transfer (constant-E) scans with $E_f = 2.9$ meV, as shown in Figs. 3(c) and 3(d). These scattering profiles are almost the same as those in the previous high-resolution inelastic neutron scattering measurements in the multi-domain state,[9] indicating that in the $(H,H,\frac{3}{2})$ line, the dispersions of the magnetic excitations in the $(1\bar{2}0)$ and $(\bar{2}10)$ domains lie above 0.5 meV.

IV. CALCULATIONS AND DISCUSSIONS

To find a set of parameters reproducing both of the single-domain spectrum and the multi-domain spectrum in
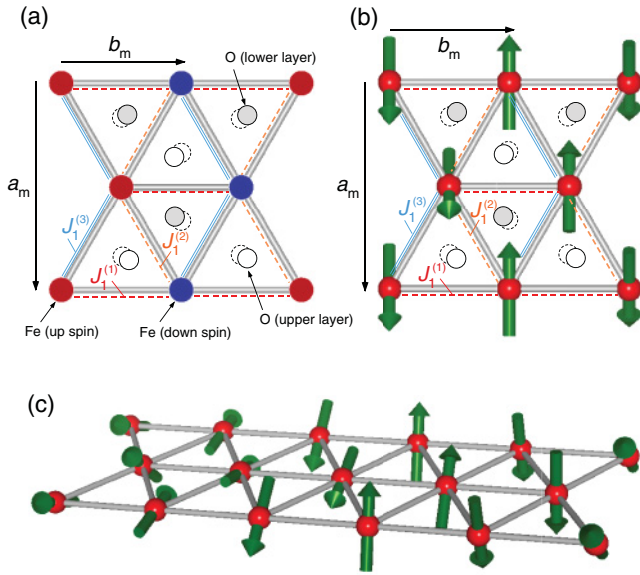
FIG. 4. (Color online) The relationship among the magnetic structure, the displacements of the oxygen ions and the nearest-neighbor exchange interactions of $J_1^{(1)}$, $J_1^{(2)}$, and $J_1^{(3)}$ in (a) the 4SL phase and (b) the multiferroic phase with the monoclinic bases. (c) Calculated spin arrangements in the multiferroic phase.

Ref. 9[18] we started from the Hamiltonian used in the previous calculation for the multi-domain spectra in the multiferroic phase:[9,10]

$$\mathcal{H} = -\frac{1}{2} \sum_{i \neq j} J_{ij} \mathbf{S}_i \cdot \mathbf{S}_j - D \sum_i \left(S_i^z \right)^2, \qquad (1)$$

in which three in-plane exchange interactions (J_1, J_2, and J_3), three interplane exchange interactions (J_{z1}, J_{z2}, and J_{z3}), a single ion uniaxial anisotropy (D), and a lattice distortion parameter (K) are employed.[9,10] The K parameter splits the nearest-neighbor exchange interactions, J_1, into two strong interactions, $J_1^{(1)} = J_1^{(2)} = J_1 - \frac{K}{2}$ and a weak interaction, $J_1^{(3)} = J_1 + K$, as shown in Fig. 4(b). It should be noted here that the application of the uniaxial pressure of 10 MPa does not result in significant changes in the magnetic-phase transition temperatures in this system.[12,13] Therefore we have considered that the Hamiltonian parameters in the slightly pressurized single-domain sample are the same as those in the multi-domain sample.

Since Fe^{3+} is $S = 5/2$, the energy can be minimized classically. Therefore, to assess the precise magnetic ground states and their energies, we employ a variational method on a large lattice of 2.0×10^4 sites, where the spin harmonics are incorporated by defining S_z within the plane as

$$S_z(\mathbf{R}) = A \left\{ \sum_{l=0} C_{2l+1} \cos[Q(2l+1) \cdot x] \right.$$
$$\left. - \sum_{l=0} B_{2l+1} \sin[(2\pi - Q)(2l+1) \cdot x] \right\}, \qquad (2)$$

where the C_{2l+1} and B_{2l+1} harmonics are produced by the anisotropy energy D and the lattice distortion K, respectively. The observed elastic intensities at odd multiples of Q and

$2\pi - Q$ are proportional to the square of these harmonics. The function $S_z(\mathbf{R})$ is normalized so that the maximum of $|S_z(\mathbf{R})|$ is $S = 5/2$. The perpendicular spin S_y is given by

$$S_y(\mathbf{R}) = \sqrt{S - S_z(\mathbf{R})^2} \, \text{sgn}[g(\mathbf{R})], \qquad (3)$$

where

$$g(\mathbf{R}) = \sin(Q \cdot x) + \frac{B_1}{C_1} \cos[(2\pi - Q) \cdot x]. \qquad (4)$$

Based on the provided magnetic ground state, the spin-wave (SW) dynamics are evaluated using a Holstein-Primakoff transformation with the spin operators given by $S_{iz} = S - a_i^\dagger a_i$, $S_{i+} = \sqrt{2S} a_i$, and $S_{i-} = \sqrt{2S} a_i^\dagger$ (a_i and $a_i^\dagger$ are bosonic destruction and creation operators). The local spin operators account for the noncollinearity through a general rotation matrix.[19,20]

The spin-wave frequencies $\omega_{\mathbf{q}}$ are determined by the equations of motion, which are solved for the vectors $\mathbf{v}_{\mathbf{q}} = [a_{\mathbf{q}}^{(1)}, a_{-\mathbf{q}}^{(1)\dagger}, a_{\mathbf{q}}^{(2)}, a_{-\mathbf{q}}^{(2)\dagger}, \ldots]$. This can be in terms of the $2N \times 2N$ matrix $\underline{M}(\mathbf{q})$ as $i d\mathbf{v}_{\mathbf{q}}/dt = -[H_2, \mathbf{v}_{\mathbf{q}}] = \underline{M}(\mathbf{q})\mathbf{v}_{\mathbf{q}}$, where N is the number of the spin sites in the large lattice employed in the present calculation, specifically 2.0×10^4.[19] The spin-wave frequencies are calculated from the condition $\text{Det}[\underline{M}(\mathbf{q}) - \omega_{\mathbf{q}}\underline{I}] = 0$, where the SW frequencies must be real and positive and all SW weights must be positive to assure the local stability of a magnetic phase.

To determine the spin-wave intensities, we examine the coefficients of the spin-spin correlation function:

$$S(\mathbf{q},\omega) = \sum_{\alpha\beta} (\delta_{\alpha\beta} - q_\alpha q_\beta) S^{\alpha\beta}(\mathbf{q},\omega), \qquad (5)$$

where α and β are x, y, or z.[21] A more detailed discussion of this method is contained in Ref. 19. The total intensity $I(\mathbf{q},\omega)$ for a constant-$\mathbf{q}$ scan is given by

$$I(\mathbf{q},\omega) = S(\mathbf{q},\omega) F_{\mathbf{q}}^2 e^{-(\omega-\omega_{\mathbf{q}})^2/2\delta^2}, \qquad (6)$$

where δ is the energy resolution and $F_{\mathbf{q}}$ is the Fe^{3+} ionic form factor, which is given as $F_{\mathbf{q}} = j_0(\mathbf{q})$, where $j_0(\mathbf{q}) = A_0 e^{a_0 s^2} + B_0 e^{b_0 s^2} + C_0 e^{c_0 s^2} + D_0$ and $s = \sin\theta/\lambda = q/4\pi$. The coefficients are $A_0 = 0.3972$ ($a_0 = 13.2442$), $B_0 = 0.6295$ ($b_0 = 4.9034$), $C_0 = -0.0314$ ($c_0 = 0.3496$), and $D_0 = 0.0044$ from Ref. 22. The simulated energy resolution is based on a Gaussian distribution, which is standard for constant-$\mathbf{q}$ scans on a triple-axis spectrometer.[23,24]

The simulated spectra, produced by the energy-minimized state for select parameters, is then compared to the observed multi-domain and single-domain spectra. The parameters are manually adjusted and the spectra are recalculated until the calculated distributions of the intensities in the $\mathbf{q}$-ω space reproduce the overall features of the observed multi-domain and single-domain spectra.

Figures 2(a) and 3(a) show the results of the calculations for the multi-domain and single-domain states, respectively. These calculations have well captured the overall features of the observed spectra. In particular, the reduction of the intensities of the shoulder around $H \approx 0.08$ in the single-domain state is successfully reproduced. This reduction is not explained by the previous Hamiltonian parameters determined only from the multi-domain spectra.[9] This demonstrates that the

TABLE I. The Hamiltonian parameters in the 4SL phase (taken from Ref. 14) and the multiferroic phase (in meV). Note that in Ref. 14, the distant interactions, J_i ($i = 2,3,z$), are also assumed to split into two J_i and J_i' owing to the monoclinic lattice distortion, although the splits are found to be relatively small ($|J_i - J_i'|/J_i \sim 0.1$). In this table, we show the mean values of them.

Composition	$J_1^{(1)}$	$J_1^{(2)}$	$J_1^{(3)}$	J_2	J_3	J_{z1}	J_{z2}	J_{z3}	D	K
CuFeO$_2$	-0.182	-0.169	-0.060	-0.041	-0.142	-0.071			0.064	0.077
CuFe$_{1-x}$Ga$_x$O$_2$ ($x = 0.035$)	-0.169	-0.169	-0.066	-0.070	-0.098	-0.070	0.014	-0.006	0.007	0.071

uniaxial-pressure control of the magnetic domain structure is highly effective to investigate the magnetic excitations in this system. The refined parameters are shown in Table I. We have found that the magnitudes of $J_1, J_2,$ and J_3 slightly decrease, on the contrary, the magnitude of J_z increases, as compared to the results of the previous analysis using only the multi-domain spectra.[9] Figure 4(c) shows the refined spin configuration, which remains almost the same as that in the previous study.[9]

We now discuss the relationship between the Hamiltonian parameters in the 4SL phase of CFO and the multiferroic phase of CFGO. As shown in Table I, the exchange interactions ($J_1^{(1)} \sim J_z$) in the 4SL and multiferroic phases are close to each other. On the other hand, the uniaxial single-ion anisotropy D in the multiferroic phase is significantly smaller than that in the 4SL phase. As was discussed in the previous works,[9,10,15] this reduction of D accounts for the change in magnetic excitations from the gapped spin-wave excitations observed in the 4SL phase to the Goldstone modes emerging from $H \approx 0.2$ and 0.3 in the multiferroic phase. Therefore this must be one of the reasons for the disappearance of the collinear 4SL magnetic ground state. However, at this moment, we have no clear explanations on the reduction of D. Further investigations to elucidate electronic states of Fe^{3+} ions in CFO and CFGO will be needed.

We subsequently focus on the small differences in exchange interactions, especially in nearest-neighbor interactions, between the 4SL and multiferroic phases. Although we could not deduce errors of the refined Hamiltonian parameters from the present analysis, we suggest the possibility that the small differences in exchange interactions can also contribute to the drastic change in the magnetic ground state, as discussed in the following.

In the previous spin-wave analysis in the 4SL phase,[14] Nakajima *et al.* have assumed that J_1 splits into three different interactions, $J_1^{(1)}$, $J_1^{(2)}$, and $J_1^{(3)}$. This assumption is based on the "scalene triangle distortion model" proposed in the synchrotron radiation x-ray-diffraction study by Terada *et al.*[25] They have observed superlattice reflections in the 4SL phase of CFO, suggesting that the equilateral symmetry of the triangular lattice is broken due to displacements of oxygen ions, as illustrated in Fig. 4(a). These displacements are explained in terms of "magnetostriction," and the resultant splitting of J_1 is expected to stabilize the 4SL magnetic order.[26] The spin-wave fitting analysis for the 4SL phase has revealed that $J_1^{(1)}$ and $J_1^{(2)}$ are comparable to each other, and are rather stronger than $J_1^{(3)}$, as shown in Table I. This relationship is similar to the splitting of J_1 in the previous theoretical works on the multiferroic phase.[9,10,27] This indicates that the effects of the

lattice distortion, namely the oxygen displacements, on the nearest-neighbor interactions can be well described by the K parameter in both of the 4SL and multiferroic phases. This is reasonable because the superlattice reflections corresponding to the displacements of the oxygen ions have been observed not only in the 4SL phase but also in the multiferroic phases.[26,28,29]

In order to quantitatively compare the effects of the lattice distortions in the 4SL and the multiferroic phases, we have estimated K and J_1 for the 4SL phase, as follows:

$$K = \left(J_1^{(3)} - \frac{J_1^{(1)} + J_1^{(2)}}{2} \right) \frac{2}{3}, \qquad (7)$$

$$J_1 = \frac{J_1^{(1)} + J_1^{(2)}}{2} + \frac{K}{2}. \qquad (8)$$

As a result, K and J_1 in the 4SL phase are estimated to be 0.077 and -0.138 meV, respectively. We found that J_1 in the 4SL phase is almost the same as that in the multiferroic phase ($J_1 = -0.140$ meV). On the other hand, the value of $K/|J_1|$, which shows the magnitude of the effect of the lattice distortion, is 0.56 in the 4SL phase; this value is slightly larger than that in the multiferroic phase ($K/|J_1| = 0.51$). This implies that the effect of the lattice distortion on J_1 is slightly weakened in the Ga-doped system. Taking account of the fact that CFO exhibits the lattice distortion in order to relieve the spin frustration, it is natural to consider that the nonmagnetic substitution, which partially releases the spin frustration, reduces the lattice distortions and their effects on the exchange interactions. In other words, the nonmagnetic substitution weakens the spin-lattice coupling in this system.

Recent theoretical studies have pointed out that strong spin-lattice coupling favors a collinear magnetic ordering.[30,31] The spin-lattice coupling in a localized spin system can be explained as a bond-length (or bonding-angle) dependence of a exchange interaction J between two spins S_i and S_j; specifically, a lattice distortion changes the energy of the bond by $-J\alpha\rho_{i,j}S_i \cdot S_j + E_{ela}$, where α is a spin-lattice coupling constant, $\rho_{i,j}$ is the change in distance between the two spins, and E_{ela} is the loss of the elastic energy due to the distortion. To maximize the energy gain due to the distortion, the value of $S_i \cdot S_j$ should be ± 1 (the $\pm$ sign depends on the signs of J, $\rho_{i,j}$, and α), and consequently the spins favor a collinear arrangement when the spin-lattice coupling is strong. From the above considerations and the present results, we suggest that the reduction of the spin-lattice coupling can be also one of the reasons for the disappearance of the collinear 4SL magnetic ground state in this system. This is consistent with the theoretical study on the CFO system by Haraldsen and Fishman; they have pointed out that the ground state

changes from the anharmonic screw-type magnetic order to the collinear 4SL magnetic order with increasing $K/|J_1|$.[10]

It is worth mentioning here that in previous synchrotron radiation measurements on CFO under applied magnetic field, Terada *et al.* have reported that the intensity of the superlattice reflection corresponding to degree of the scalene triangular lattice distortion starts to decrease at the magnetic-field induced phase transition from the 4SL phase to the multiferroic phase.[29] This implies that the spin-lattice coupling also plays an important role in the magnetic-field induced phase transitions in the CFO system.

We should also mention the distant interactions. As seen in Table I, there are small differences in the values of J_2 and J_3 between the multiferroic phase and the 4SL phase, although the relationship of $J_3 > J_2$ holds in both of the phases. This might be because J_{z2} and J_{z3} are neglected in the spin-wave analysis in the 4SL phase in Ref. 14. Another possibility is the effect of the monoclinic lattice distortion. Nakajima *et al.* have pointed out that the monoclinic lattice distortion affects the distant exchange interactions, although this effect is relatively small as compared to the effect of the oxygen displacements on J_1.[14] Because the previous x-ray-diffraction studies have revealed that the degree of the monoclinic distortion in the 4SL phase is larger than that in the multiferroic phase,[29,32] the difference in the monoclinic lattice constants could be the reason for the differences in J_2 and J_3.

V. CONCLUSION

We have performed inelastic neutron scattering measurements on a multiferroic CFGO ($x = 0.035$) in order to refine the Hamiltonian parameters in the multiferroic phase. By applying a uniaxial pressure of 10 MPa onto the [1$\bar{1}$0] surfaces of the single-crystal CFGO sample, we have produced a nearly single-domain multiferroic phase. We have successfully observed the magnetic excitation spectrum in the single-domain state. Using the Hamiltonian employed in the previous inelastic neutron scattering study on a multi-domain multiferroic phase of CFGO ($x = 0.035$),[9] we have refined the Hamiltonian parameters so as to simultaneously reproduce both of the observed single-domain and multi-domain spectra. Comparing the refined Hamiltonian parameters in the multiferroic phase with those in the collinear 4SL magnetic ground state of undoped CFO,[14] we have found that the single-ion uniaxial anisotropy D is significantly reduced and the lattice distortion parameter K is slightly reduced by the nonmagnetic substitution. Although the disappearance of the collinear 4SL magnetic ground state can be mainly ascribed to the reduction of D, we have suggested that the reduction of the spin-lattice coupling, which reflects the partial release of the magnetic frustration due to the nonmagnetic substitution, can also contribute to the emergence of the noncollinear incommensurate magnetic ground state.

*nakajima@nsmsmac4.ph.kagu.tus.ac.jp

[1] T. Kimura, J. C. Lashley, and A. P. Ramirez, Phys. Rev. B **73**, 220401(R) (2006).

[2] S. Mitsuda, H. Yoshizawa, N. Yaguchi, and M. Mekata, J. Phys. Soc. Jpn. **60**, 1885 (1991).

[3] S. Seki, Y. Yamasaki, Y. Shiomi, S. Iguchi, Y. Onose, and Y. Tokura, Phys. Rev. B **75**, 100403(R) (2007).

[4] S. Kanetsuki, S. Mitsuda, T. Nakajima, D. Anazawa, H. A. Katori, and K. Prokes, J. Phys.: Condens. Matter **19**, 145244 (2007).

[5] N. Terada, T. Nakajima, S. Mitsuda, H. Kitazawa, K. Kaneko, and N. Metoki, Phys. Rev. B **78**, 014101 (2008).

[6] E. Pachoud, C. Martina, B. Kundys, C. Simona, and A. Maignana, J. Solid State Chem. **183**, 344 (2009).

[7] T. Nakajima, S. Mitsuda, S. Kanetsuki, K. Prokes, A. Podlesnyak, H. Kimura, and Y. Noda, J. Phys. Soc. Jpn. **76**, 043709 (2007).

[8] T. Nakajima, S. Mitsuda, K. Takahashi, M. Yamano, K. Masuda, H. Yamazaki, K. Prokes, K. Kiefer, S. Gerischer, N. Terada *et al.*, Phys. Rev. B **79**, 214423 (2009).

[9] J. T. Haraldsen, F. Ye, R. S. Fishman, J. A. Fernandez-Baca, Y. Yamaguchi, K. Kimura, and T. Kimura, Phys. Rev. B **82**, 020404(R) (2010).

[10] J. T. Haraldsen and R. S. Fishman, Phys. Rev. B **82**, 144441 (2010).

[11] F. Ye, J. A. Fernandez-Baca, R. S. Fishman, Y. Ren, H. J. Kang, Y. Qiu, and T. Kimura, Phys. Rev. Lett. **99**, 157201 (2007).

[12] T. Nakajima, S. Mitsuda, T. Nakamura, H. Ishii, T. Haku, Y. Honma, M. Kosaka, N. Aso, and Y. Uwatoko, Phys. Rev. B **83**, 220101 (2011).

[13] T. Nakajima, S. Mitsuda, T. Haku, K. Shibata, K. Yoshitomi, Y. Noda, N. Aso, Y. Uwatoko, and N. Terada, J. Phys. Soc. Jpn. **80**, 014714 (2011).

[14] T. Nakajima, A. Suno, S. Mitsuda, N. Terada, S. Kimura, K. Kaneko, and H. Yamauchi, Phys. Rev. B **84**, 184401 (2011).

[15] R. S. Fishman, J. Appl. Phys. **103**, 07B109 (2008).

[16] T. R. Zhao, M. Hasegawa, and H. Takei, J. Cryst. Growth **166**, 408 (1996).

[17] N. Aso, Y. Uwatoko, H. Kimura, Y. Noda, Y. Yoshida, S. Ikeda, and S. Katano, J. Phys.: Condens. Matter **17**, S3025 (2005).

[18] We have used the multi-domain spectrum shown in Ref. 9 to compare with the present calculations, while there are no remarkable differences between the multi-domain spectrum in Ref. 9 and that in the present work.

[19] J. T. Haraldsen and R. Fishman, J. Phys.: Condens. Matter **21**, 216001 (2009).

[20] M. E. Zhitomirsky and I. A. Zaliznyak, Phys. Rev. B **53**, 3428 (1996).

[21] G. L. Squires, *Introduction to the Theory of Thermal Neutron Scattering* (Dover, New York, 1978).

[22] A. Dianoux and G. Lander, *Neutron Data Booklet* (OCP Science, Philadelphia, 2003).

[23] G. Shirane, S. M. Shapiro, and J. M. Tranquada, *Neutron Scattering with a Triple-Axis Spectrometer* (Cambridge University Press, Cambridge, England, 2002).

[24] N. J. Chesser and J. D. Axe, Acta Crystallogr., Sect. A **29**, 160 (1973).

[25] N. Terada, S. Mitsuda, H. Ohsumi, and K. Tajima, J. Phys. Soc. Jpn. **75**, 023602 (2006).

[26] N. Terada, S. Mitsuda, Y. Tanaka, Y. Tabata, K. Katsumata, and A. Kikkawa, J. Phys. Soc. Jpn. **77**, 054701 (2008).

[27] R. S. Fishman and S. Okamoto, Phys. Rev. B **81**, 020402 (2010).

[28] T. Nakajima, S. Mitsuda, T. Inami, N. Terada, H. Ohsumi, K. Prokes, and A. Podlesnyak, Phys. Rev. B **78**, 024106 (2008).

[29] N. Terada, Y. Tanaka, Y. Tabata, K. Katsumata, A. Kikkawa, and S. Mitsuda, J. Phys. Soc. Jpn. **75**, 113702 (2006).

[30] K. Penc, N. Shannon, and H. Shiba, Phys. Rev. Lett. **93**, 197203 (2004).

[31] F. Wang and A. Vishwanath, Phys. Rev. Lett. **100**, 077201 (2008).

[32] N. Terada, Y. Narumi, Y. Sawai, K. Katsumata, U. Staub, Y. Tanaka, A. Kikkawa, T. Fukui, K. Kindo, T. Yamamoto *et al.*, Phys. Rev. B **75**, 224411 (2007).

[33] K. Momma and F. Izumi, J. Appl. Crystallogr. **41**, 653 (2008).